PAPER • **OPEN ACCESS**

Effect of patch geometry and resin type on mechanical properties of repairing deep scratch damage to aircraft composites

To cite this article: Muharrem Er *et al* 2025 *Mater. Res. Express* **12** 085305

Materials Research Express

PAPER

Effect of patch geometry and resin type on mechanical properties of repairing deep scratch damage to aircraft composites

Muharrem Er[1,*], **Can Çivi**[2,*], **Raif Sakin**[3,*] and **Gökhan Eyici**[2]

[1] National Defense University, Army NCO Vocational HE School, Department of Aircraft Technology, Balıkesir, Turkiye
[2] Manisa Celal Bayar University, Faculty of Engineering and Natural Sciences, Department of Mechanical Engineering, Manisa, Turkiye
[3] Balıkesir University, Edremit Vocational High School, Department of Machine and Metal Technologies, Balıkesir, Turkiye
[*] Authors to whom any correspondence should be addressed.

E-mail: muharrem.er@msu.edu.tr, can.civi@cbu.edu.tr and rsakin@balikesir.edu.tr

Keywords: composite aircraft structure, repair process, thermoset resin, continuous glass-roving, deep scratch damage

OPEN ACCESS

RECEIVED
14 April 2025

REVISED
6 August 2025

ACCEPTED FOR PUBLICATION
13 August 2025

PUBLISHED
26 August 2025

Abstract

This study investigated the effects of patch geometry and resin type on mechanical properties in repairing small damages, such as deep scratches, on the exterior surfaces of composite components, such as fuselages, wings, tail stabilizers, and aircraft doors. A handheld prototype device was developed to impregnate glass roving with epoxy resin and apply a repair filler to damaged areas. To simulate the fuselage outer layer, 6 twelve-layer 2–3 mm thick composite plates ($V_f \approx 55\%$) were produced by hot pressing using Duratek® epoxy and 300 g m^{-2} woven glass fabric. Tensile and flexural samples were prepared from plates per standard. U and V cross-section artificial scratch damage was created on samples with 40% of their thickness using two milling cutter types on a CNC router, resulting in three test samples: undamaged and two damage types. Three epoxy resins (Loctite®, Duratek®, and Polisan®) were applied to the U and V damaged areas with a handheld device, and 6–9 layers of filling patches were made using impregnated 300 tex glass roving. The repaired samples were cured at 23 °C for 24 h, under an infrared lamp at 40 °C for 4 h, and at 60 °C for 2 h. Tensile and flexural tests on the original and repaired samples showed a tensile strength recovery of up to 94%, tensile modulus of 89%, flexural strength of 65%, and flexural modulus of 99%. The U-patched samples demonstrated higher tensile and flexural strengths than the V-patches, with Duratek® epoxy proving advantageous for tensile properties and Loctite® for flexural properties.

1. Introduction

Composite materials used in the aircraft industry are classified as fiber-reinforced composites and layered composites (sandwich composites/honeycomb) according to the shapes and placement of the reinforcement elements and as polymer matrix and metal matrix composites according to the matrix material [1, 2]. In aircrafts, fiber-reinforced composite materials are used in primary structural components, such as fuselages, wings, tail stabilizers, and doors. The frequency of minor accident damage is high throughout an aircraft's operating life, and its repair has a significant impact on maintenance costs. In conventional mechanical joining processes, such as the screwing of thermoplastic and thermoset composite materials, delamination problems due to stresses formed during drilling, corrosion between the material and fastener, and deformation occurring in the composite material are undesirable features. This has led to the development of simultaneous curing, bonding, and secondary bonding techniques as alternatives to the mechanical joining methods in the aircraft industry. Owing to its small stress concentration, good appearance, and light weight, adhesive repair has attracted significant attention in aviation and aerospace fields [3].

Patch repairs are based on bonded/glued connections that transmit loads and are therefore one of the most effective elements of repair quality. The patch repairs of aircraft composites are gaining increasing importance in the repair of damaged parts owing to their time savings rather than cost savings, as well as their applicability to complex geometric components. In the repair of medium and large damages of these composite components,

Table 1. Effect of patch geometry and resin type on repair performance in some literature.

Patch shape/resin type	Strength recovery	Durability/damage resistance	References
Rectangular/epoxy	High	High	[17–19]
Circular/epoxy	Medium-high	Low damage area	[20, 21]
Elliptical/epoxy	High	Low stress concentration	[21, 22]
Scarf/thermoplastic resin	Very high (at optimum)	High	[21, 23]
Hybrid/reinforced resin	Very high	High delamination resistance	[24]

usually due to impact; bonding methods and patch geometries such as scarf, stepped scarf, double curved and bonded scarf, additional patch and stepped lap have been suggested [4–8]. Conversely, significant efforts have been devoted to studying bonded repair methods and the performance of fiber-reinforced composites. The most important goal of repairing damaged composite materials with patches is to increase the original strength of the material as much as possible after the repair. For instance, Li *et al* [9] produced a large number of carbon fiber/epoxy composite sheets with holes of the same size, repaired the sheets with patches of various geometries, and subjected them repaired and undamaged samples to tensile testing. As a result of the test, they concluded that the tensile strength of the patch-repaired samples improved by 5%–16% compared to that of the undamaged sample, depending on the patch shape. Psarras *et al* [10] evaluated the mechanical properties of carbon fiber reinforced polymer composites (CFRP) by repairing the damaged areas with a weft patch (stepped, U-V sectioned patch), and observed that the tensile strength of the samples was recovered by 65%–69% after the repair in their study. Şişman and Ramazanoğlu [11] repaired elliptically damaged glass fiber-reinforced composite panels using single-sided lap joints with glass fiber-reinforced composite patches of different sizes and numbers of layers, and the repaired samples were subjected to tensile loads. The patched samples carried up to 145% more tensile load than the damaged ones. Feng *et al* [12] investigated the flexural behavior of patch-repaired aircraft winglets and showed that the repaired winglets retained approximately 82% of the load-bearing capacity of the intact winglets. In the literature, different repair processes are recommended for the damage to composite panels used in aircraft components. Hamoush *et al* [13] studied repair patches of solid laminated composites, including circular disbond and fiber mismatching between the patch and the parent material. Their results showed that both defective and good repairs restored the strength to 80% of that of intact panels. Wang *et al* [14] investigated the effect of surface defects and patches created in different geometries on the bending properties of the composite plate. They proved that the U-type scratch opened by providing a radius of half the crack width to the sharp edges had a higher retention rate than rectangular and V-type scratches with a relatively smaller radius. Hu and Soutis [15] showed that composite plates repaired with the external patching method could keep an average of 68.75% of their original strength, while Breitzman *et al* [16] proved that they could retain up to 90% of their strength with prepreg repair applied to the damaged area. Some recent studies on the effect of patch geometry and resin type on repair performance are presented in table 1.

As can be seen from the previous studies mentioned above, no repair geometry recommendations were found for damage other than small, deep scratches (less than 2.0 mm) on plastic sheets, such as acrylic, in general aircraft maintenance, and applications of advanced composite materials in aircraft and composite repair engineering case study handbooks [25–27]. In addition, only a few researchers at different times have investigated the bonding, patching, and repair processes for minor damages, such as deep scratches. In their study, Shams and El-Hajjar [28, 29] examined the repair of deep surface scratches and cracks in continuous carbon fiber/epoxy laminated composites. Initially, they filled the interior of the open patch channel with a fiber-free resin and subsequently applied a prepreg-type woven fabric adhesive repair patch to the damaged region. They then conducted numerical and experimental investigations on the top-layer repair of scratch damage in composite laminates. The specimens with only resin filled into the deep scratches achieved the strength of the original panels by 54.4%. In comparison, the specimens with a 5 mm wide single layer patch on the resin met the strength target by 67.4%, and the specimens with two-layer patches met the strength target by 99.5%. In this study, a damage repair prototype was developed for small deep scratch-type damage of composite surfaces used in aircraft. Analyses and examinations were conducted to establish the relationship between the change in the patch structure and the strength of the patch process carried out using this prototype.

2. Materials and methods

The study has two basic steps: developing a new and original patch application prototype to carry out the composite repair process and performing patch processes on artificially damaged composite samples using this prototype. In this study, an E-glass woven fabric with an areal density of 300 g m^{-2} was used as the fiber to produce composite plates, and Duratek® DTE1000 epoxy resin was used as the matrix. Single-end roving

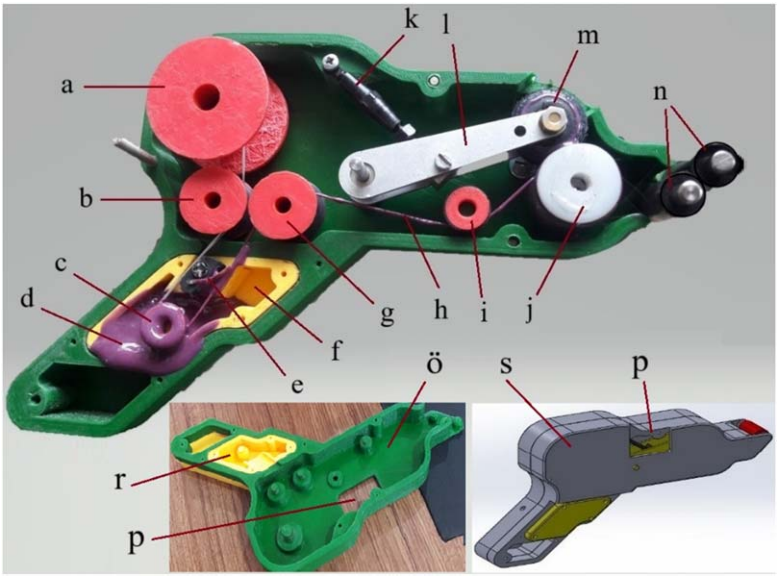

a) fiber winding reel
b, c, g and i) tension reels
d) resin
e) scraper mechanism
f) resin tank
h) resin-impregnated fiber
j) motor drive reel
k) adjustable tension mechanism
l) pressure mechanism arm
m) pressure wheel
n) patch surface pressure wheel
o) symmetry main body
p) adjustment window
r) tank filling cover
s) 3D image

Figure 1. Hand-held patching device prototype.

Table 2. Mechanical and physical properties of E-glass woven fabric and glass-roving [33].

Properties	E-glass woven fabric	Single-end roving
Areal density (g m^{-2})	300	—
Linear density (g/1000 m)	—	300 tex
Density (g m^{-3})	2.54	2.54
Fiber diameter (μm)	12–17	13.75
Tensile strength (MPa)	2300	1270
E-modulus (GPa)	69–82	28.34
Poisson's ratio	0.22	0.22
Ultimate elongation (%)	2.97	4.83

Table 3. Some properties of resins used in the patch [30–32].

Properties	Epoxy resins		
	Loctite®	Duratek®	Polisan®
Hardener/resin ratio	22%	25%	33%
Density (g m^{-3})	1.15	1.10	1.12
Viscosity (Pa.s)	150–300	0.95	2.85
Tensile strength (MPa)	32.2	71–76	31.53
E-modulus (GPa)	2303	3.1–3.4	N/A
Ultimate elongation (%)	10.0	4.0–4.5	N/A

(WR 6), which is used in filament winding applications and is a product of Şişecam Glass Fiber Company (Türkiye), was used to patch the damaged plates. As patch matrix, three different two-component commercial epoxies, namely Loctite® EA9309.3NA (USA) [30], Duratek® DTE1000 (Türkiye) [31] and Polisan® (Türkiye) [32] were used together with appropriate hardeners, respectively. The properties of the woven E-glass fabric and glass roving are listed in table 2 and those of the epoxy resins are listed in table 3.

2.1. Design of a hand-held patching device

In the first phase of the study, a handheld prototype was developed for the repair of damaged composite structures. Each part of the device was drawn in 3D using the SolidWorks program on a 1/1 scale. In this device, as shown in figure 1, a glass fiber rope consisting of approximately 750–800 fibers with a diameter of 14 μm on the winding reel (a) with a linear density of 300 g/1000 m and a tensile strength of 1270 MPa passes through the

Figure 2. Composite plate manufacturing by hot-pressing.

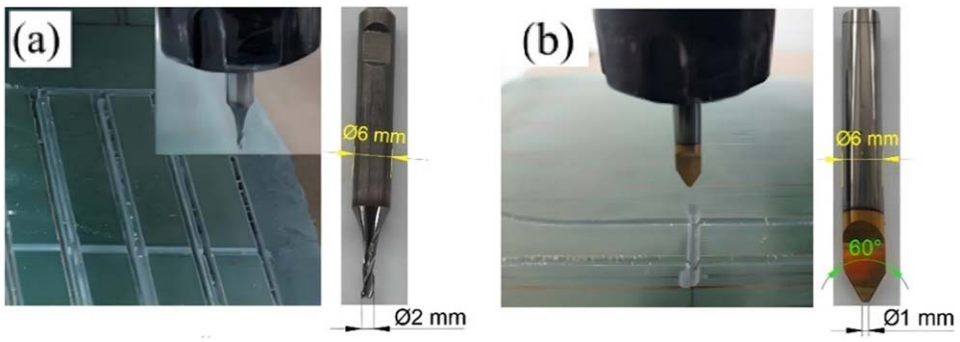

Figure 3. Artificial damage created by (a) U- and (b) V-sections and milling cutters used in the process.

inner surface of the tension reel (b) at a moving speed of 312 mm min^{-1} under the effect of the tensile force applied by the motor drive reel (j) and the pressure wheel (m) connected to the DC motor, and passes through the tank inlet channel and around the tension reel (c) inside the tank. The fiber wetted with resin inside the tank exits from the resin scraping mechanism (e) and the tank outlet channel, passes around the tension reels in (g) and (i) between the pressure wheel (m) and the motor drive reel (j), and exits the device between the surface pressure wheels (n). Thus, a damaged composite plate can be repaired by patching with resin-impregnated fibers.

2.2. Manufacturing of the composite plates

In the second phase, six composite plates ($V_f \approx 55\%$) were produced from 300 g m^{-2} glass-woven fabric with 12 layers, dimensions of 270 × 360 mm, and thickness of 2–3 mm using the hand lay-up and hot-pressing method. These plates are similar to the composite exterior components of aircrafts, such as fuselages, wings, tail stabilizers, and doors. For this purpose, the glass fabrics were first impregnated with Duratek® epoxy in accordance with the hand lay-up method, and then laid on top of each other in the metal lower mold cavity. The upper mold was then closed, and as shown in figure 2, the laminates in the metal mold were cured in a 60-ton press at 100 °C and 30 bar pressure for 4 h. The heater was then switched off and the plates were left to cool under constant pressure for 24 h.

Tensile samples were cut from the composite plates according to the TS EN ISO 527-4 standard [34], whereas flexural samples were cut according to ASTM-D7264/D7264M [35]. Both types of samples were cut from the plates using a three-axis mini CNC router (Hattech Company, Bursa, Turkey) with a spindle speed of 18000 rpm and a feed rate of 300 mm min^{-1}. As illustrated in figure 3, U- and V-section scratches (artificial damage) were opened in tensile samples, 10 mm along the sample width, and in bending samples, 13 mm along the sample width. These damages are called deep scratches with U- and V-geometries, respectively. Two different end mills were used to cut deep scratches. One had a tungsten carbide tip with a diameter of 2 mm and three flat sides for U-geometry. The other end mill had a cobalt-coated tip with a diameter of 1 mm and two sides angled at 60° for V-geometry. The artificial scratches created by milling were introduced into the samples at a depth of 40% (0.8–1.2 mm) of their thickness. The milling process was completed with automatic feed in 8–12

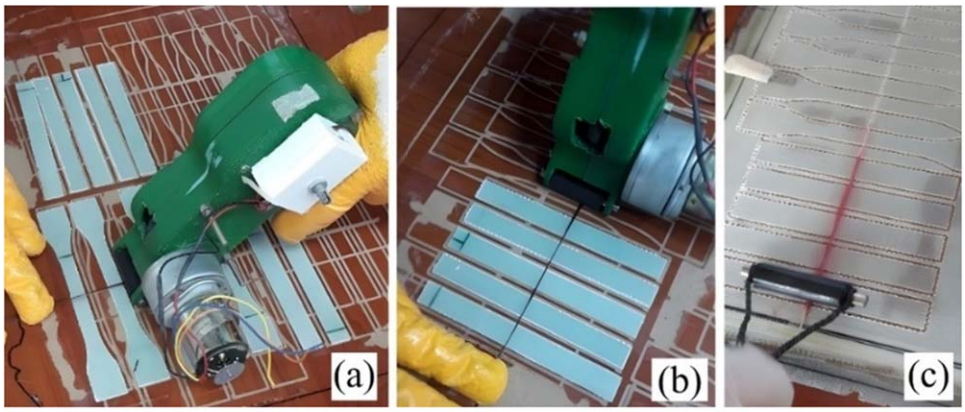

Figure 4. Patching of specimens and applying external pressure to the patch.

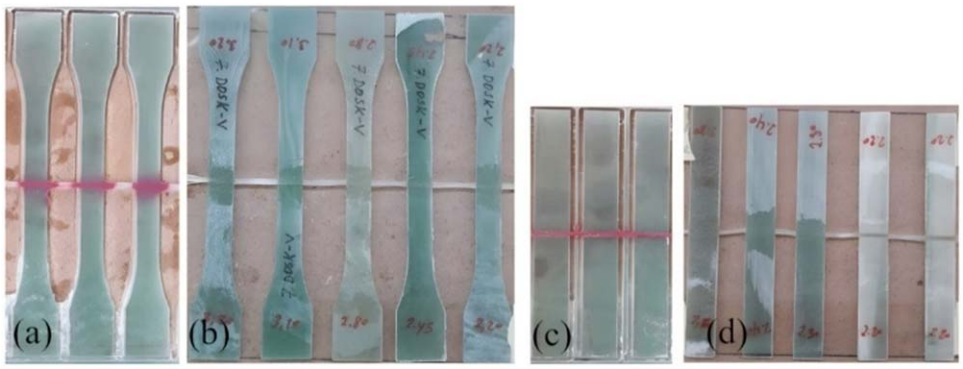

Figure 5. Tensile and flexural specimens cured at 23 °C/24 h.

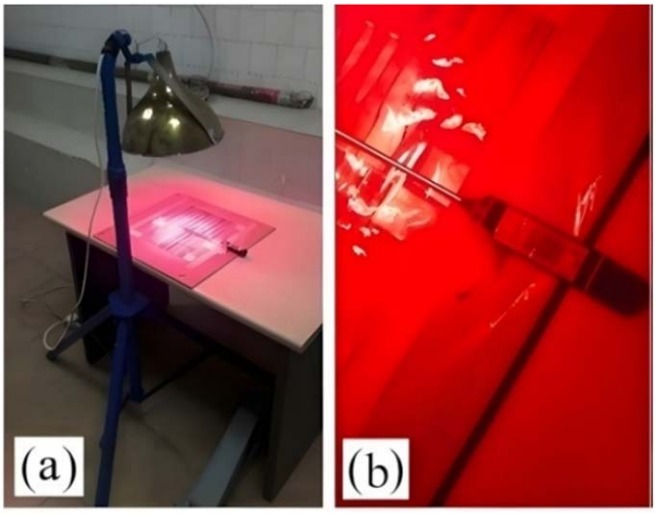

Figure 6. (a) IR curing unit, and (b) curing of samples.

steps, cutting 0.1 mm deep at each step. Thus, the artificial damage was sustained up to the fifth layer of the twelve-layer composite samples. This process resulted in the creation of two distinct root gaps on the composite plates, characterized as U- and V-shaped sections, prior to the application of the patching procedure.

2.3. Roughness measurement of scratch side surfaces (SS)

Increasing the surface roughness in patching processes results in an increase in bond strength, primarily owing to mechanical interlocking and expansion of the surface area [36–39]. For example, in fiber-reinforced epoxy

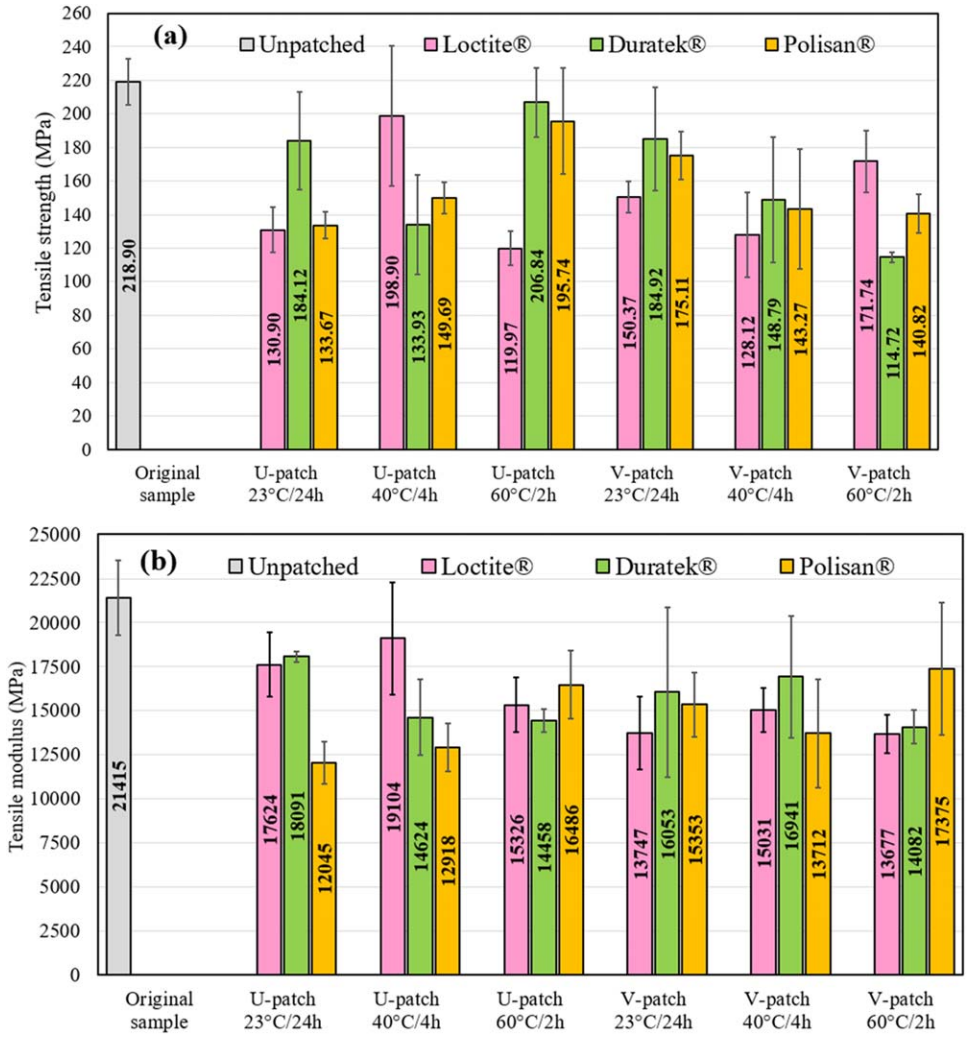

Figure 7. Results of (a) tensile strength, and (b) tensile modulus.

Table 4. Test results of original and unpatched samples.

Original samples		U-shaped scratched specimens			V-shaped scratched specimens		
σ_{to} (MPa)	E_{to} (MPa)	σ_{tu} (MPa)	E_{tu} (MPa)	k	σ_{tv} (MPa)	E_{tv} (MPa)	k
218.9	21415	95.2	13135	2.299	106.2	12454	2.061
σ_{fo} (MPa)	E_{fo} (MPa)	σ_{fu} (MPa)	E_{fu} (MPa)	k	σ_{fv} (MPa)	E_{fv} (MPa)	k
361.0	21961	210.8	13013	1.712	191.9	12447	1.881

composites, an increase in surface roughness is associated with an increase in the adhesion interfacial shear strength (IFSS) [39, 40]. As a result, roughness values, particularly on the side surfaces of the bond, are crucial for the patch efficiency and strength. This is because the adhesion side surfaces of the U- and V-scratches were the main surfaces that carried the stresses acting on the specimen. A Sunpoc SRT310 digital surface-roughness measuring device was used for this purpose.

2.4. Patching of artificially deep-scratched specimens and curing

The plates with artificial deep scratch damage were first patched with a handheld device, designed and prototyped in the first stage, by filling with continuous glass roving with three different epoxies, as described above (figures 4(a) and (b)). Simultaneously, the first compression was performed on a still wet patch with a compression wheel in the device. The areas patched with the device were compressed for a second time by pressing them with an external Teflon-based roller (figure 4(c)). Patching with the composite filler was repeated

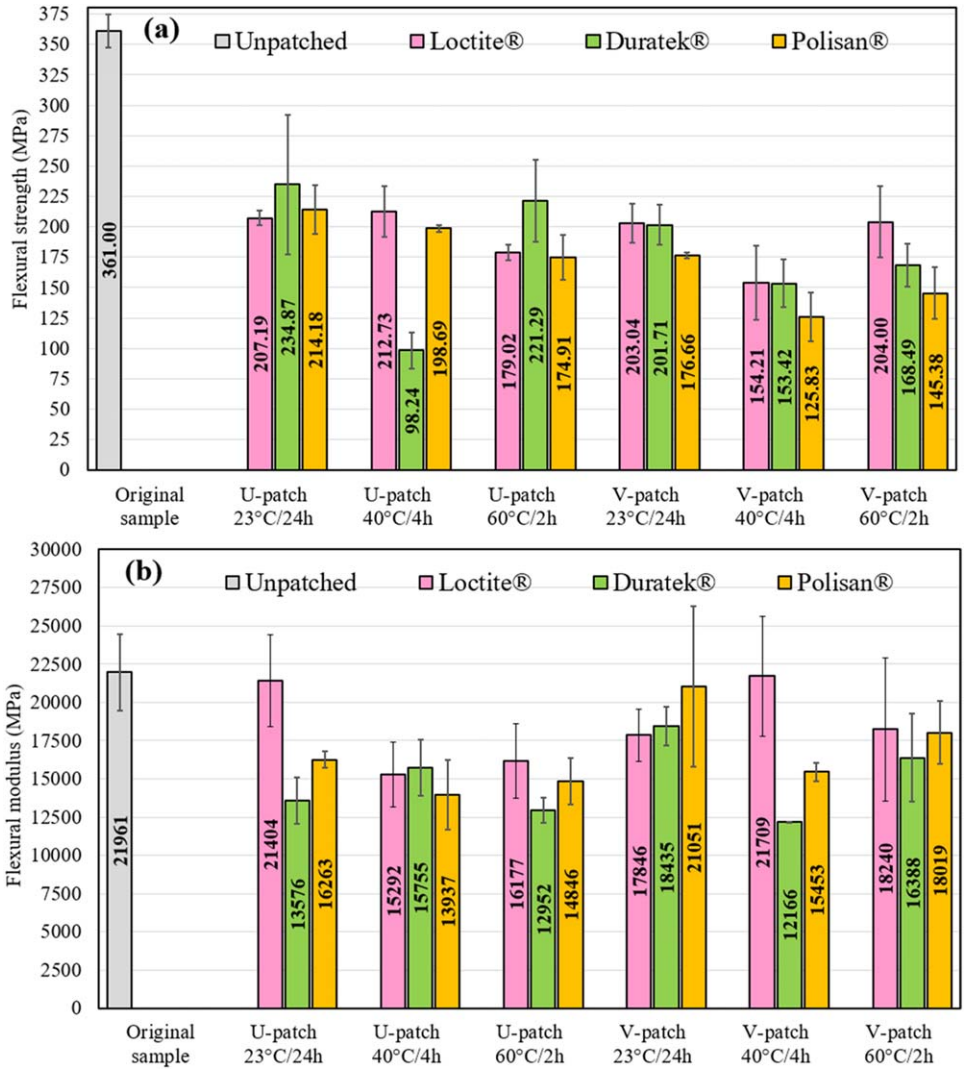

Figure 8. Results of (a) flexural strength, and (b) flexural modulus.

(6–9 times) until the deep scratches were covered ($V_f \approx 40\%$). Subsequently, the composite samples with the repair filling were cured under various conditions. These conditions included a room temperature of 23 °C for 24 h (figure 5), 40 °C with a 250 W infrared lamp for 4 h, and 60 °C for 2 h (figure 6).

2.5. Tensile and three-point bending tests

Tensile and three-point flexural tests were applied to the original, damaged, and patched samples using three different epoxies in a 100 kN testing machine (Schimatzu AG-IS 100 kN). The tensile and three-point bending tests were conducted at a rate of 1.0 mm min^{-1}. Ten specimens of the original samples were subjected to tensile and bending tests. Two distinct deep scratches were applied to the surface of the composite sample, and their repair was conducted under three different epoxy types and curing conditions. Thus, 18 distinct repair scenarios were used. At least three to four specimens were tested for each scenario. To examine the effect of the patch process in detail, stereo microscopy and SEM images were obtained from the surfaces of the samples damaged during the tests. Stereo microscope images were obtained using a Tignapoo 7' screen 2000X digital microscope. SEM images were obtained using a Quanta FEG 250 SEM device.

Another investigation carried out within the scope of this study was the calculation of stress concentration for the relevant structures. Stress concentration is primarily caused by the sudden deformation or discontinuity of materials, such as cracks or holes. Fracture initiation occurs at the point of stress concentration, which is the primary factor leading to material failure. The stress concentration factor was calculated using equation (1) [14, 41, 42]:

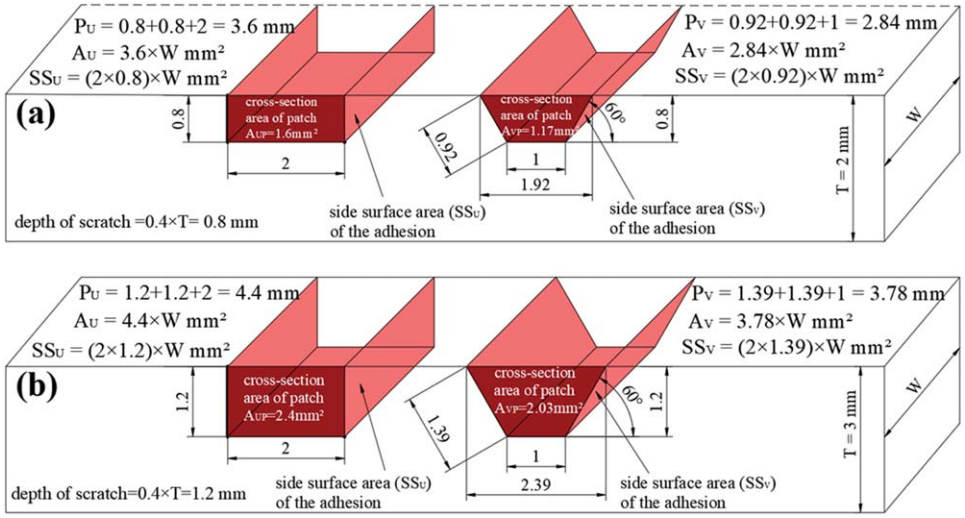

Figure 9. Patch geometries and dimensions; (a) scratch depth of 0.8 mm and (b) 1.2 mm.

$$k = \frac{\sigma_{\max}}{\sigma_{nom}} \tag{1}$$

where k is the factor of stress concentration, and $\sigma_{\max}$ is the maximum stress, and σ_{nom} is the nominal stress.

3. Results and discussion

In this study, the effects of three distinct factors on the performance of U- and V-patches were examined: (1) patch geometry and stress concentration factor depending on patch geometry, (2) resin type (viscosity and strength), and (3) roughness of adhesion surfaces

The tensile and flexural properties of the original and unpatched specimens are listed in table 4 and those of the patched specimens are shown in figures 7 and 8, respectively. The symbols in table 4 are defined as follows: σ_{to}, tensile strength; E_{to}, tensile modulus; σ_{fo}, flexural strength; E_{fo}, flexural modulus; and k is the stress concentration factor. Furthermore, σ_{tu} and σ_{tv} are the tensile strengths; E_{tu} and E_{tv} are the tensile moduli; σ_{fu} and σ_{fv} are the flexural strengths; and E_{fu} and E_{fv} are the flexural moduli of the unpatched U- and V-shaped scratched specimens, respectively.

As shown in figures 7 and 8, the samples repaired using the developed process recovered an original tensile strength of up to 94%, tensile modulus of 89%, flexural strength of 65%, and flexural modulus of 99%. It is thought that the reason why the bending modulus of the samples repaired with the developed process can meet the original at a rate of 99% is due to the fact that 'the bonding side surface area (SSV) in the V-geometry is 15.0%–15.8% larger than the U-geometry (SSU)' as expressed in figure 9. It was understood that the cracks formed on the patch/scratch bonding side surfaces in the V-patched samples 'reach the weak interfaces more quickly through the 60° slip planes in the main plate layers and facilitate the general damage with delamination damage' compared to the U-patched samples. The maximum tensile strength of the repaired samples could be attained by creating a U-geometry and curing the patched area with Duratek® epoxy at 60 °C using an infrared lamp for 2 h. The maximum flexural strength was achieved by utilizing Duratek® epoxy in the U-geometry and Loctite® epoxy in the V-geometry, with the patched area cured with an infrared lamp at 60 °C for 2 h.

3.1. Effect of the patch geometry and stress concentration factor

Factors affecting patch strength include patch adhesion surface area and cross-sectional volume [43, 44]. The average tensile strength, tensile modulus, and flexural strength of the U-patched samples were 7%, 3.5%, and 13.6% higher than those of the V-patched samples, respectively (figures 7–8). The reasons for this were understood when both the total surface area and cross-section of the patch region were calculated mathematically. According to figure 9, the total adhesion surface area ($A_U = P_U \times W$ and $A_V = P_V \times W$) of the U-geometry, including the bottom surfaces, was 16.4%–26.7% larger than that of the V-geometry. Similarly, the U-section area (A_{UP}) of the patches was 18.2%–36.7% larger than that of the V-section (A_{VP}). By contrast, the average flexural modulus of the V-patched samples was 14% higher than that of the U-patched samples. This is because the adhesion side surface area in the V-geometry (SS_V), which accommodates the stresses, is 15.0%–15.8% larger than that in the U-geometry (SS_U), as illustrated in figure 9. Therefore, for the U-scratch, the stress

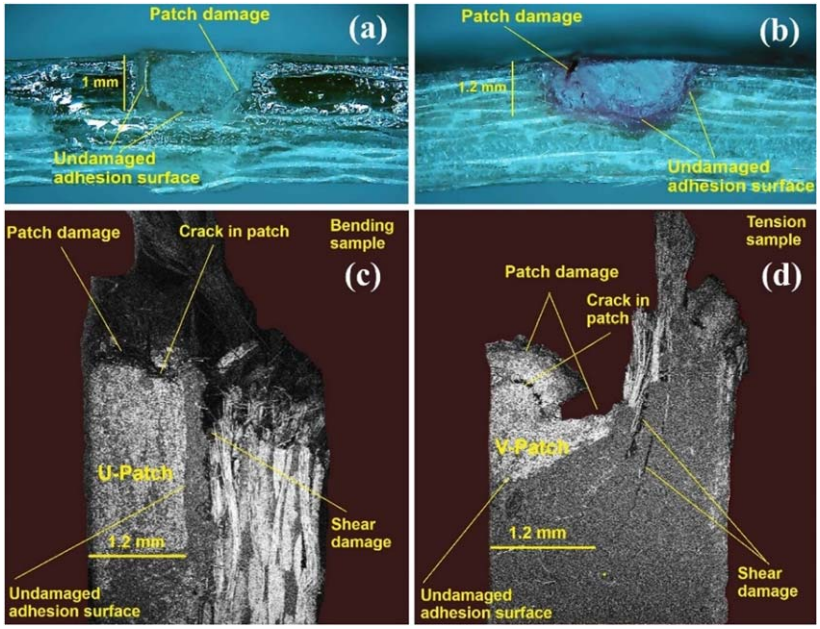

Figure 10. Damaged images of U- and V-patch flexural samples; (a) fracture on patch surface, (b) separation on the right-side adhesion surface, (c) undamaged adhesion surface (SEM), and (d) separation on the right and left side adhesion surface (SEM).

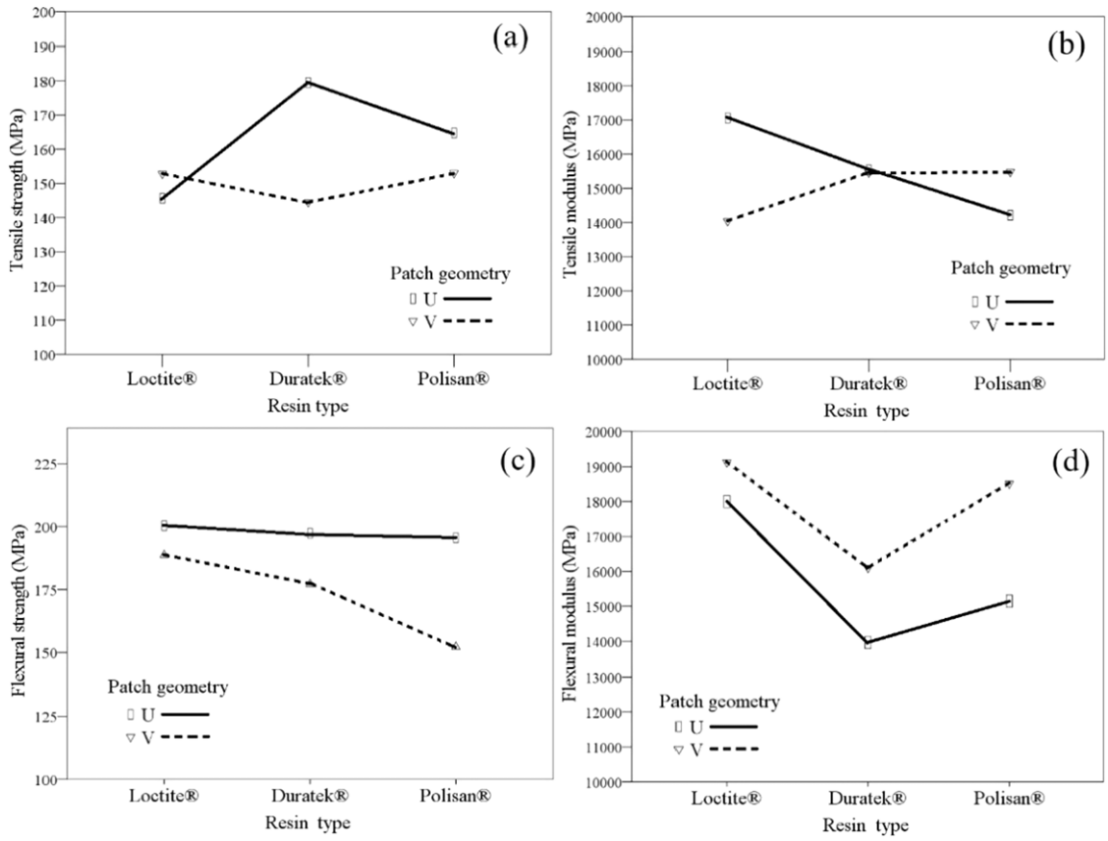

Figure 11. Variation of mechanical properties depending on resin type and patch geometry.

concentration factor (k) was 1.712, whereas for V-scratch, it was 1.881 (table 4). Therefore, U-scratch damage carries less stress, is less prone to fracture, and has a higher strength than V-scratch damage, regardless of the patch.

Compared to the U-patched samples, the cracks formed on the side surfaces of the patch adhesion in the V-patched samples reached the weak interfaces more quickly through the 60° shear planes in the main plate

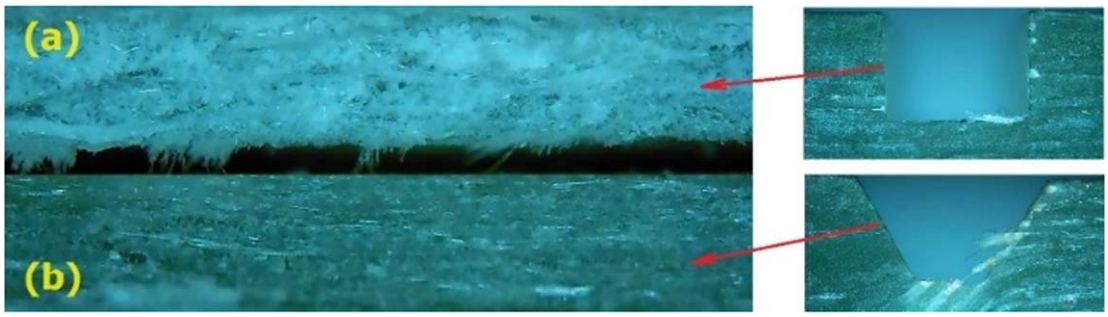

Figure 12. Images of side surfaces of the adhesion for unpatched specimens; (a) U- and (b) V-shaped scratches.

Figure 13. SEM images of fracture surfaces in the U and V patches.

layers and facilitated general damage with delamination damage (figure 10). This reduced the strength of the V-patch filler and its ability to adhere to the surface during flexural stress.

3.2. Effect of the resin type

As shown in figure 11, the strength values vary depending on the type of resin and geometry of the patch.

When the viscosity values of the epoxies used in the patching process are examined in table 3, it is seen that the lowest viscosity value is in Duratek® ($\mu_{Dur} = 0.95$ Pa.s), followed by Polisan® ($\mu_{Pol} = 2.85$ Pa.s), and the highest is in Loctite® ($\mu_{Loc} = 150$–300 Pa.s). The viscosity value indicates the fluidity of the epoxy and its ability to wet the fibers. Epoxies with low viscosity exhibit superior adhesion properties because of their ability to wet the fibers and layers better. When the effects of the resin type and patch geometry were evaluated, the strength values of the resins were Duratek® ($\sigma_{çDur} = 71$–76 MPa), Loctite® ($\sigma_{çLoc} = 32.2$ MPa), and Polisan® ($\sigma_{çPol} = 31.53$ MPa) (table 3). Therefore, Duratek was more advantageous when the tensile properties were compared. The fact that the tensile strength and modulus of the composites patched with Duratek® are higher than those of the other composites seems reasonable in terms of both resin viscosity and resin strength. For this reason, the average tensile strength of the samples patched with Duratek® is 8.7% higher than Loctite® and 2.2% higher than Polisan®, regardless of the patch geometry and curing conditions (figure 11(a)). In terms of tensile modulus, Loctite® has a negligible advantage, and the average tensile modulus of the samples patched with Loctite® is 0.3% higher than Duratek® and 4.7% higher than Polisan® (figure 11(b)). In terms of flexural properties, the Loctite® patch appeared to be more advantageous. The average flexural strength and modulus of the samples patched with Loctite® were 4.0% and 23.5% higher than those of Duratek® and 11.8% and 10.3% higher than those of Polisan®, respectively (figures 11(c) and (d)).

3.3. Effect of the roughness of the patch surfaces

In the machining of composites, the number of cutting edges of the cutting tool and roughness of the machined surface are directly proportional [45]. A cut-off length of 0.8 mm was employed for each roughness measurement, and an evaluation (sampling) length of 4 mm (5×0.8 mm) was set in accordance with the ISO

Table 5. Comparison of some key parameters in this study with those in other studies.

Patch Geometry (shape)	Method	Fiber	Matrix or adhesive	Recovery rate of mechanical properties (%)				References
				Tensile		Flexural		
				σ_t	E_t	σ_f	E_f	
square (▣), circle (◎) and hexagonal (⬢)	Double-sided external patch	Carbon prepreg	Epoxy	5–16	N/A	N/A	N/A	[9]
rectangular ▣)	Stepped scarf (ply-by-ply)	Carbon prepreg	Epoxy	65–69	92–96	N/A	N/A	[10]
rectangular ▣)	One-sided external patch	Glass cloth	Epoxy	38	N/A	N/A	N/A	[11]
circle (◎)	Stepped scarf (ply-by-ply)	Carbon prepreg	Epoxy	N/A	N/A	82	N/A	[12]
circle (◎)	Stepped scarf (ply-by-ply)	Carbon cloth	Epoxy	80–95	N/A	N/A	N/A	[13]
circle arc (∪), square (⊔) and triangle (⋁)	One-sided external patch	Carbon prepreg	Ni-based solder	N/A	N/A	54–69	N/A	[14]
square (⊔)	One-sided external patch	Carbon prepreg	Ti-based solder	N/A	N/A	69–92	N/A	[47]
circle (◎)	Double-sided external patch	Carbon cloth	Araldite epoxy	68–69	N/A	N/A	N/A	[15]
circle (◎)	Stepped scarf (ply-by-ply)	Carbon prepreg	Epoxy	85–90	N/A	N/A	N/A	[16]
triangle (⋁)	Covering the damage with fibercloth	Carbon prepreg	Epoxy	67–99	74–117	N/A	N/A	[28, 29]
rectangular (⊔) and half hexagonal ▽)	Filling with continuous glass fiber impregnated with resin	Single end glass roving	Epoxy	84–94	79–89	61–65	84–99	This study

σ_t: tensile strength (MPa), E_t: tensile modulus (MPa), σ_f: flexural strength (MPa), E_f: flexural modulus (MPa).

4287-1 standard [46]. For the U-scratch surface (SS_U), $R_a = 3.253 \pm 0.423$ μm and $R_{max} = 28.190 \pm 4.732$ μm; for the V-scratch surface (SS_V), $R_a = 1.699 \pm 0.075$ μm and $R_{max} = 14.510 \pm 0.814$ μm were measured (figure 12).

The tool used to open the U-scratch had three cutting edges, whereas the tool with two cutting edges was used for the V-scratch (figure 3). Therefore, the roughness of the U-scratched surface was approximately 1.9 × higher than that of the V-scratched surface (figure 12). When the SEM images of the fracture surfaces in the U and V patches in figure 13 were examined, it was observed that the V-patch was more easily peeled off from the composite plate against the applied load, and the fibers in the patch remained clearly in the middle. On the other hand, the U-patch is seen to resist the load more because of better adhesion, and the fiber traces in the patch are not clear. Surfaces with higher porosity, rougher and more obvious fiber ends that are subject to discontinuity in the main composite component provide better adhesion of the patch filler.

4. Conclusion

Within the scope of this study, a prototype patch device was developed to repair deep scratch damage for composite surfaces used in aircrafts. The key parameters in this study were compared with those in other studies (table 5). As shown in table 5, previous studies have primarily examined the tensile strength and modulus to determine the recovery rate of repaired composite materials. However, in this study, the recovery of the tensile and flexural strengths, as well as the tensile and flexural moduli, was also examined and compared with the literature. Additionally, analyses were performed on the patch processes that could be performed using the relevant device. In general, the following key conclusions were reached.

- The mechanical properties of the specimens repaired through the process developed in this study exhibited satisfactory improvements compared to those of the original specimens. This enhancement was contingent upon factors such as the patch geometry, epoxy type, and curing conditions.
- The stress concentration factor of the U-geometry is lower than that of the V-geometry. Therefore, U-geometry damage carries less stress, is less prone to fracture, and has a higher strength than V-geometry damage regardless of the patch. Consequently, sharp-cornered steps, grooves, or sections should be avoided as much as possible in patch geometries, and circular arc transitions should be used for sudden shape changes.
- The increase in the patch geometry and roughness of the adhesion surfaces increases the strength of the repaired sample in direct proportion.
- Although the increase in resin viscosity reduced the tensile strength of the repaired sample, the increase in resin strength also increased the sample strength. Therefore, Duratek® is advantageous in terms of its tensile properties. The fact that the tensile strength and modulus of the composites patched with Duratek® were higher than those of the others is logical in terms of both resin viscosity and resin strength. In terms of flexural properties, the Loctite® patch appeared to be more advantageous.

Acknowledgments

This study was supported by the Balıkesir University Scientific Research Projects Coordination Unit (project numbers 2020/082 and 2020/084).

Data availability statement

All data that support the findings of this study are included within the article (and any supplementary files).

Ethical statement

Not applicable.

References

[1] Alçı M 2016 Investigation on low velocity impact behavior of nomex honeycomb sandwich structures reinforced by laminated composite plates *MSc Thesis* Institute of Natural Sciences, Department of Mechanical Engineering, Kayseri Erciyes University
[2] Yılmaz U and Evci C 2015 Future of composite materials in aerospace and defense industry *The Journal of Defense Sciences* **14** 77–109

[3] Dahmen V, Redmann A J, Austermann J, Quintanilla A L, Mecham S J and Osswald T A 2020 Fabrication of hybrid composite T-joints by co-curing with 3D printed dual cure epoxy *Composites Part B: Engineering* **183** 107728
[4] Budhe S, Banea M and de Barros S 2018 Bonded repair of composite structures in aerospace application: a review on environmental issues *Applied Adhesion Science* **6** 1–27
[5] Archer E and McIlhagger A 2020 Repair of damaged aerospace composite structures, book in *Polymer Composites in the Aerospace Industry* (Elsevier) 441–59
[6] Zhou W, Ji X-l, Yang S, Liu J and Ma L-h 2021 Review on the performance improvements and non-destructive testing of patches repaired composites *Compos. Struct.* **263** 113659
[7] Katnam K B, Da Silva L and Young T 2013 Bonded repair of composite aircraft structures: a review of scientific challenges and opportunities *Prog. Aerosp. Sci.* **61** 26–42
[8] USA-Deptpartment-of-Defense 1997 Composite materials handbook *Materials, Usage, Design, and Analysis.* 3 of 5 (CRC Press)
[9] Li C, Zhao Q, Yuan J, Hou Y and Tie Y 2019 Simulation and experiment on the effect of patch shape on adhesive repair of composite structures *J. Compos. Mater.* **53** 4125–35
[10] Psarras S, Loutas T, Galanopoulos G, Karamadoukis G, Sotiriadis G and Kostopoulos V 2020 Evaluating experimentally and numerically different scarf-repair methodologies of composite structures *Int. J. Adhes. Adhes.* **97** 102495
[11] Şişman A and Ramazanoğlu M 2023 The effect of patching properties on tensile stress behaviours in the repair of composite plates *Journal of Science, Technology and Engineering Research* **4** 1–8
[12] Feng W, Xu F, Li M, Zhang X and You H 2018 Experimental investigation of repair of impact-damaged aircraft winglet under static bending moments *J. Adhes. Sci. Technol.* **32** 1410–27
[13] Hamoush S, Shivakumar K, Darwish F, Sharpe M and Swindell P 2005 Defective repairs of laminated solid composites *J. Compos. Mater.* **39** 2185–96
[14] Wang W, Fu Q, Sun J, Zhang P and Hu D 2022 The mechanical and repair behavior of damaged carbon/carbon composites *Ceram. Int.* **48** 22759–66
[15] Hu F and Soutis C 2000 Strength prediction of patch-repaired CFRP laminates loaded in compression *Compos. Sci. Technol.* **60** 1103–14
[16] Breitzman T, Iarve E, Cook B, Schoeppner G and Lipton R 2009 Optimization of a composite scarf repair patch under tensile loading *Composites Part A: Applied Science and Manufacturing* **40** 1921–30
[17] Mohammed S M K, Mhamdia R, Albedah A, Bouiadjra B A B, Bouiadjra B B and Benyahia F 2021 Fatigue crack growth in aluminum panels repaired with different shapes of single-sided composite patches *Int. J. Adhes. Adhes.* **105** 102781
[18] Salem M, Berrahou M, Mechab B and Bouiadjra B B 2021 Analysis of the adhesive damage for different patch shapes in bonded composite repair of corroded aluminum plate under thermo-mechanical loading *J. Fail. Anal. Prev.* **21** 1274–82
[19] Gangadharan S and Sv B 2016 Impact Analysis of composite repair patches of different shapes at low velocities for aircraft composite structures *J. Aeronaut. Aerosp. Eng.* **5** 1000173
[20] Shankar S V and Idapalapati S 2023 Effect of scarf repair geometry on the impact performance of aerospace composites *Polymers* **15** 2390
[21] Vadean A, Abusrea M, Shazly M, Michel A, Kaabi A and Boukhili R 2023 Improvement of scarf repair patch shape for composite aircraft structures *The Journal of Adhesion* **99** 1044–70
[22] Xing R, Wang F, Yang Y and Li G 2024 Optimization of composite material repair patch shape based on strength analysis *Applied Sciences* **14** 4397
[23] Khan T, Hafeez F and Umer R 2023 Repair of aerospace composite structures using liquid thermoplastic resin *Polymers* **15** 1377
[24] Venkatesan D B and Vellayaraj A 2024 The effect of adhesively bonded external hybrid patches on the residual strength of repaired glass/epoxy-curved laminates *Polym. Compos.* **45** 3493–506
[25] USA_Deptpartment_of_Army 1992 *Technical Manual, Aviation Unit Maintenance (AVUM) and Aviation Intermediate Maintenance (AVIM) Manual for General Aircraft Maintenance (Sheet Metal Shop Practices)* 10 (Headquarters, Department of the Army)
[26] Steiner B M, Peltier J R, Janny S J and Cerovsky B A 2023 *Composite Repair Engineering Case Studies for US Army Aerostructures* SR-FCDD-AMR-23-01 U.S. Army Combat Capabilities Development Command, Aviation & Missile Center (https://doi.org/(Accessed on: 10 April 2025) https://apps.dtic.mil/sti/html/trecms/AD1208761)
[27] USA_Deptpartment_of_Army 2013 *General Aircraft Maintenance, Advanced Composite Material General Maintenance and Practices (TM 1-1500-204-23-11)* 11 (Headquarters, Department of the Army)
[28] Shams S S and El-Hajjar R F 2013 Overlay patch repair of scratch damage in carbon fiber/epoxy laminated composites *Composites* A **49** 148–56
[29] Shams S S and El-Hajjar R F 2015 Repair: adhesive repair for surface gouges and cracks in continuous carbon fiber/epoxy laminated composites *Joining Composites with Adhesives: Theory and Applications* 173
[30] Loctite®/EA9309.3NA. EA 9309.3NA AERO Epoxy Paste Adhesive (known as Hysol EA 9309.3NA) (Accessed on: 24 November 2023) https://heatcon.com
[31] Duratek®/DTE1000. DTE1000 DTS1100 Epoxy Resin (Accessed on: 10 September 2024) (https://company.metstrade.com)
[32] Polisan®. Polisan solvent-free, two-component, reaction-curing epoxy resin (Accessed on: 02 February 2024) (https://tdsapp.polisankansai.com/en/pdf/view/658fbfcd25f2f50010ab7a4b/tr/webpage)
[33] Sakin R 2017 Effects of glass-mat on mechanical anisotropy in bidirectional e-glass woven roving reinforced composite sheets produced by RTM method *Pamukkale University Journal of Engineering Sciences* **23** 967–73
[34] TS-EN-ISO-527-4 2007 *Determination of Tensile Properties—Part 4: Test Conditions for Isotropic and Orthotropic Fibre-Reinforced Plastic Composites* (Turkish Standards Institute)
[35] ASTM-D7264/D7264M 2007 *Standard Test Method for Flexural Properties of Polymer Matrix Composite Materials* (USA, Book) 19428-2959
[36] Osouli-Bostanabad K, Tutunchi A and Eskandarzade M 2017 The influence of pre-bond surface treatment over the reliability of steel epoxy/glass composites bonded joints *Int. J. Adhes. Adhes.* **75** 145–54
[37] Yang G, Yang T, Yuan W and Du Y 2019 The influence of surface treatment on the tensile properties of carbon fiber-reinforced epoxy composites-bonded joints *Composites* B **160** 446–56
[38] Kwon D-J, Kim J-H, Kim Y-J, Kim J-J, Park S-M, Kwon I-J, Shin P-S, DeVries L K and Park J-M 2019 Comparison of interfacial adhesion of hybrid materials of aluminum/carbon fiber reinforced epoxy composites with different surface roughness *Composites* B **170** 11–8
[39] Song W, Gu A, Liang G and Yuan L 2011 Effect of the surface roughness on interfacial properties of carbon fibers reinforced epoxy resin composites *Appl. Surf. Sci.* **257** 4069–74

[40] Liang Y-C, Zhang X-H, Wei X-H, Jing D-Q, Su W-G and Zhang S-C 2023 Contribution of surface roughness and oxygen-containing groups to the interfacial shear strength of carbon fiber/epoxy resin composites *New Carbon Mater.* **38** 1116–26
[41] Pilkey W D, Pilkey D F and Bi Z 2020 *Peterson's Stress Concentration Factors* (Wiley)
[42] Güldü İ, Dağhan B and Kaya S 2003 An investigation of stress concentration in filleted GRP composite plates *Dokuz Eylül University Faculty of Engineering Journal of Science and Engineering* **5** 27–35
[43] Gad M M, Rahoma A, Khan Z A, Al-Thobity A M, Abualsaud R, Alkaltham N, Akhtar S, Ateeq I S and Al-Harbi F A 2022 Closed repair technique: innovative surface design for polymethylmethacrylate denture base repair *Journal of Prosthodontics* **31** 257–65
[44] Gama B A, Mahdi S, Cichanowski C, Yarlagadda S and Gillespie J J W 2004 *Static and dynamic strength of scarf-repaired thick-section composite plates DAAD19-01-2-0005* Center for Composite Materials, University of Delaware Army Research Laboratory, Aberdeen Proving Ground https://apps.dtic.mil/sti/pdfs/ADA427494.pdf (Accessed on: 10 April 202 5)
[45] Duboust N, Ghadbeigi H, Pinna C, Ayvar-Soberanis S, Collis A, Scaife R and Kerrigan K 2017 An optical method for measuring surface roughness of machined carbon fibre-reinforced plastic composites *J. Compos. Mater.* **51** 289–302
[46] ISO-4287 1997 *Geometrical Product Specifications (GPS) - Surface texture: Profile method - Terms, Definitions and Surface Texture Parameters* (International Standards Organization)
[47] Wang W, Hu J, Tang Y and Fu Q 2025 Improving flexural performance of repaired C/C composites through Ti addition: mechanism analysis *J. Alloys Compd.* **1010** 177339